

Two-dimensional system - black phosphorus: electronic, atomic structure and transport properties of bP(100) single crystals

Ionov A. M., Zagitova A. A., Bozhko S. I., Kulakov V. I., Zverev V. N.

Institute of Solid State Physics, Russian Academy of Sciences, 142432, Moscow Region, Chernogolovka, st. Academ. Osipyana.

Abstract – The electronic, atomic structure and transport properties of black phosphorus (bP) single crystals prepared by high-pressure methods and a gas-transport reaction were studied by X-ray photoelectron spectroscopy (XPS) and scanning probe microscopy (STM, AFM). After exposure of the clean surface under atmospheric conditions, the features in the XPS spectra corresponding to the oxidized form of phosphorus were observed. The appearance of oxidized areas on the surface was also detected using AFM. The atomic resolution of the surface of a single crystal was obtained by the STM method. As a result of low-temperature transport measurements, impurity activation energies were determined, and negative magnetoresistance along the Y direction was detected.

1. INTRODUCTION

Recently, in condensed-matter physics, greater attention has been paid to systems with reduced dimensionality. Two-dimensional materials, quantum threads, quantum dots, as well as various hybrid structures based on them, attract the attention of scientists for the reason that their properties often differ from those of a bulk material. Among two-dimensional materials, graphene, dichalcogenides of transition metals, hexagonal boron nitride, and monoatomic layers of Si, Ge, Sn have also been extensively studied.

2D materials are thin sheets of atomic thickness that exhibit exotic physical and mechanical properties with promising potential for technological applications and fundamental science. So far, most conventional 2D materials have been derived from a limited set of bulk solids consisting of stacked, weakly bound sheets (graphite, MoS₂, hexagonal boron nitride, and black phosphorus).

The simplest examples exist in elemental 2D materials, of which two are known to also occur in a bulk layered form: graphite (graphene) and 2D black phosphorus (phosphorene).

Phosphorus demonstrates multiple bulk allotropes such as highly reactive white phosphorus, red phosphorus and purple phosphorus, and relatively inert black phosphorus. 2D phosphorus, or phosphorene, is among the few 2D materials isolated directly from a bulk solid, specifically from black phosphorus. Black phosphorus exhibits an orthorhombic crystal structure composed of stacked, weakly bound layers. However, these layers are buckled out of the plane to form corrugated rows, resulting in significant anisotropy in mechanical strength, electrical and thermal conductivity, and optical properties. As a promising two-dimensional material, black phosphorus was also proposed which is the allotropic modification of phosphorus most stable under normal conditions [1, 2, 3].

Black phosphorus is a layered material where atomic layers are held by weak van der Waals forces. Atomic layers of bP have a "corrugated" structure, and are not flat, as, for example, in graphene. The lattice belongs to orthorhombic syngony, pr. Cmca, $a = 4.37$, $b = 3.31$, $c = 10.47$ Å. The distance between the layers is 5.3 Å. In the black phosphorus

monolayer, two types of bonds are present: a short bond of the order of 2.224 Å connects the nearest P in one plane, a longer bond at 2.244 Å connects the upper and lower atoms of one layer [4].

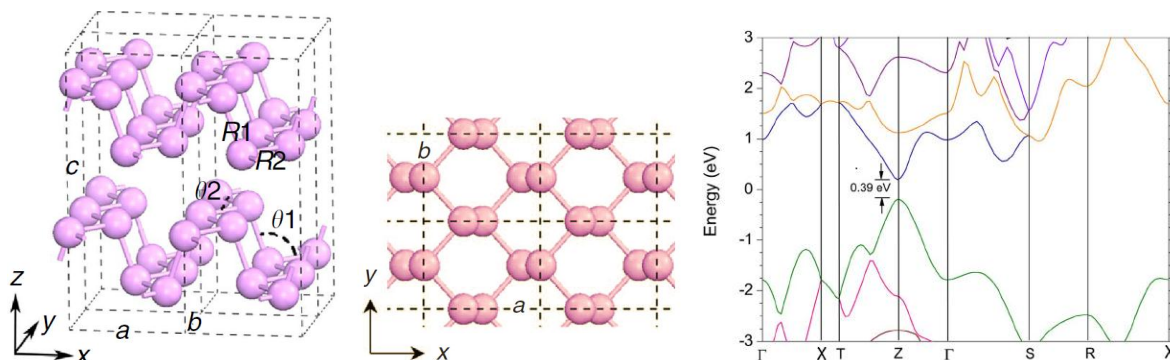


Fig.1: Crystal structure of black phosphorus [2]. Electronic structure of bulk phosphorus [11].

The anisotropic structure of bP, which determines its anisotropic electrical, thermal, optical, and mechanical properties, distinguishes it favorably among other two-dimensional materials. The first experiments to measure the electrical conductivity were carried out on polycrystalline samples [5, 6, 7, 8] during which black phosphorus was determined as a p-type direct-band semiconductor with a band gap of 0.33-0.35 eV. According to the theoretical calculations [9, 10, 11] in bP, the minimum of the conduction band and the maximum of the valence band (VB) are located at the point Z (Fig. 1). With a decrease in the number of layers, the width of the forbidden band at the point T increases and for phosphorene, according to various theoretical calculations, reaches 1.5-2 eV.

The material remains a direct-gap semiconductor, which distinguishes it, for example, from dichalcogenides of transition metals where the forbidden zone becomes indirect with the decreasing number of layers. The size of the forbidden band experimentally measured by scanning tunneling microscopy was 2.05 eV [12].

The first methods of obtaining black phosphorus crystals differed in their increased toxicity and did not allow the synthesis of large single crystals [13, 14, 15]. The method of gas transport reaction [16, 17, 18] produced single crystals, but the results varied greatly depending on the synthesis conditions, and the crystal growth mechanisms have not been fully revealed yet. Therefore, one of the tasks of the work was to prepare larger single crystals of black phosphorus. Further, the morphology, atomic and electronic structure of the obtained crystals surface, and low-temperature measurements of the electrical conductivity and magnetoresistance of the samples were studied.

2. RESULTS

Single crystals of bP were obtained by two methods. In the high pressure method, red phosphorus was placed in the pyrophyllitic ampoule of a container for high pressure, the synthesis was carried out at the pressure $P=1.1$ GPa and temperature $T=860$ °C. In the gas-transport reaction method, the starting materials - red phosphorus, AuSn and SnI_4 - were placed into a 10 cm-long quartz ampoule at $p=10^{-2}$ torr and kept at the temperature $T=590$ °C. The temperature gradient at the length of the ampoule was 10-20 °C, single crystals of black phosphorus grew on the colder end of the ampoule for 5 days. The crystals obtained had an orthorhombic syngony (cf. Cmca, $a=4.37$, $b=3.31$, $c=10.47$ Å), the X-ray data confirmed crystallinity of the samples (Fig. 2).

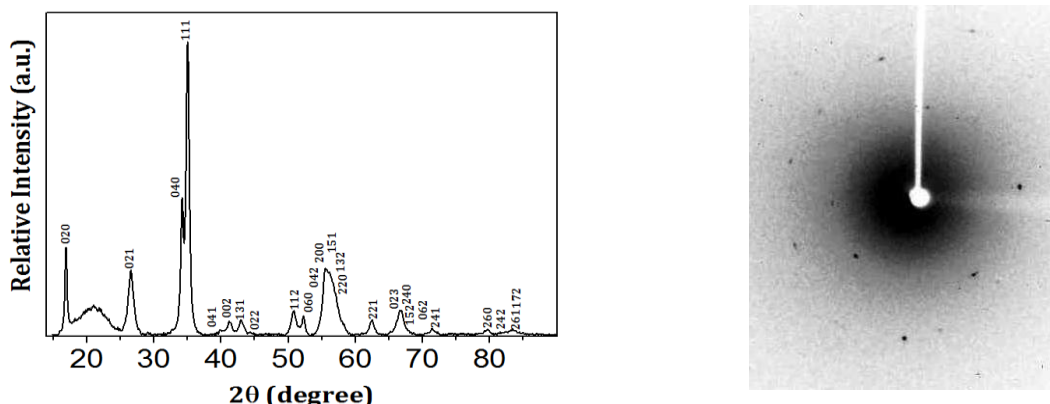


Fig. 2: a) Diffractogram of black phosphorus crystals, b) X-ray axial pattern of the crystal.

The analysis of the electron microscope images (Fig. 3) showed that crystals with characteristic dimensions of $10\mu\text{m} \times 20\mu\text{m}$ were obtained by the method of high pressure, while those of the crystals obtained using the gas transport reaction method were $1\text{mm} \times 100\mu\text{m}$. The crystal growth during the gas-transport reaction occurred along the Y direction.

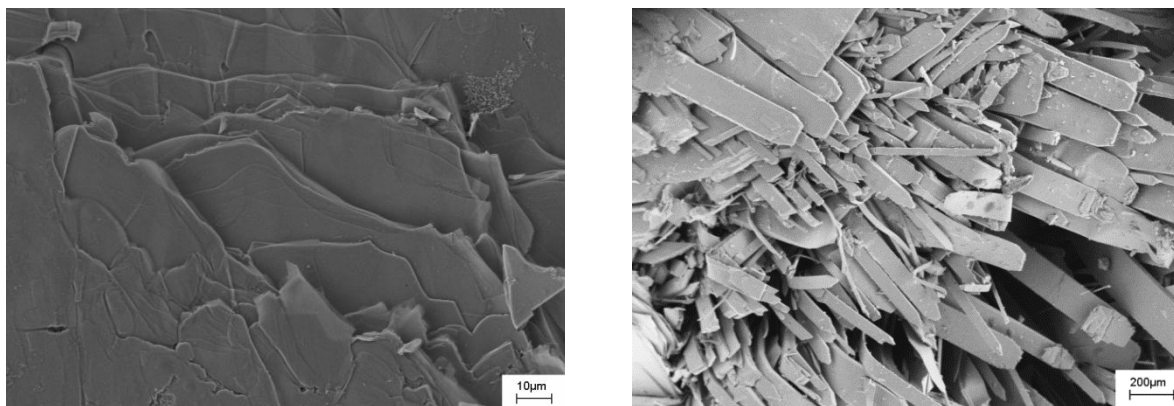


Fig. 3: SEM images of bP crystals obtained by the method of: a) high pressure, b) gas transport reaction.

The investigation of the surface morphology and atomic structure was carried out by STM methods in ultrahigh vacuum and AFM in the air. The image of bP surface, obtained by STM, is presented in Fig. 4a. The sample was split by sticky tape in vacuum of 10^{-8} Torr, in the analysis chamber the pressure was 10^{-10} Torr. Surface topography was studied at $U_{\text{bias}} = 0.6\text{V}$, $I = 100\text{pA}$, it was possible to obtain atomic resolution at room temperature. The two-dimensional Fourier transform of the STM image shows the presence of a long-range order. The lattice parameters $a = 4.66$ and $b = 2.75\text{\AA}$ obtained from the analysis of the Fourier image are close to the experimental values of the parameters obtained from X-ray diffraction analysis.

The difference in the STM values can be explained by the temperature drift of the sample which leads to distortion of the STM image (the STM image and its Fourier image are elongated along the X axis, corresponding to the axis of slow scanning of the STM). The reflex in 2.4\AA in the FFT image reflects periodicity of the structure, which agrees

with the bond length of 2.22\AA between the phosphorus atoms [4]. Figure 4b shows the tunnel spectra recorded in four different sections of the sample. The performed measurements enabled estimating qualitatively the value of the gap which was $0.3\text{--}0.35\text{ eV}$, which agrees with the literature data for bP [3, 5].

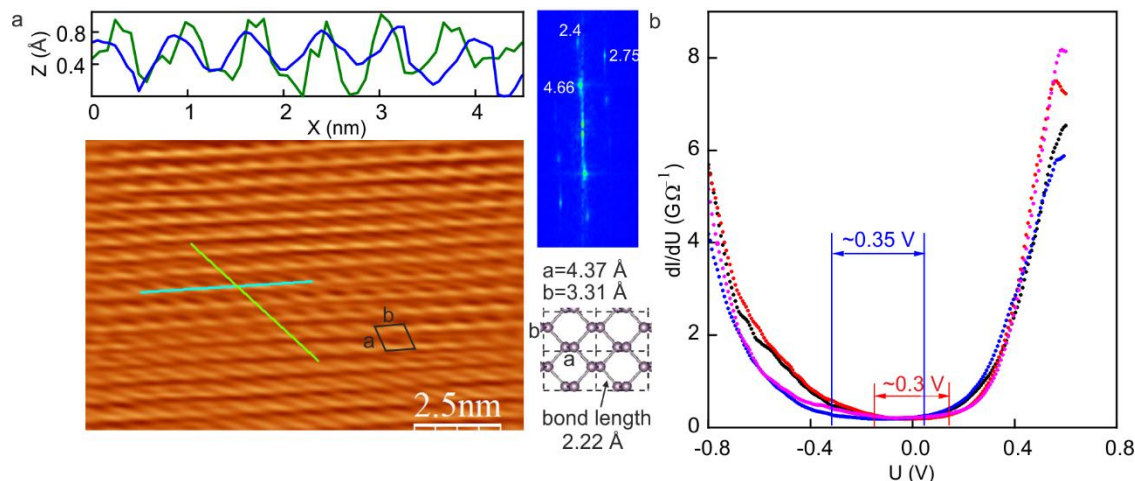


Fig. 4: a) STM image of the P(100) surface (insets: profiles along the lines, Fourier image of the STM image (reflexes are indicated in \AA), image of the unit cell), b) STS spectra taken at four different points.

The elemental composition of the P(001) surface and the electronic structure were investigated by XPS using $\text{AlK}\alpha$ radiation ($h\nu = 1486.6\text{ eV}$). An overview of the XPS spectrum of the bP surface is shown in Fig. 5a. The spectrum of the core levels of P2s and P2p, characteristic of pure phosphorus, as well as the traces of oxygen O1s and C1s, is observed. No foreign impurities were found on the surface of black phosphorus after the synthesis.

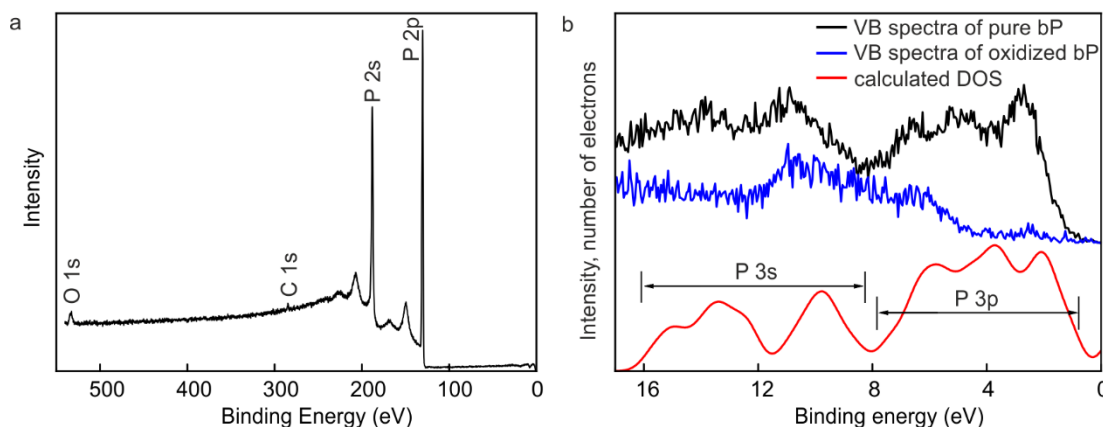


Fig. 5: a) Overview XPS spectrum of the bP(100) surface synthesized by high pressure method after etching, b) VB spectra of pure and oxidized phosphorus and calculated DOS.

It was of interest to study the chemical stability of the black phosphorus surface under various conditions. For this purpose, the XPS spectra of a clean surface obtained by argon ions etching under ultrahigh vacuum conditions and the surface of a sample aged under atmospheric conditions for a period from several hours to 100 days were taken. In the XPS spectrum of the pure sample, there is a spin-orbit doublet ($\text{P}2p_{1/2}$ and $\text{P}2p_{3/2}$ with binding energies of 131.1 and 130.2 eV (Fig. 6a) characteristic of pure phosphorus.

Exposure of the sample in the air led to a shift of the doublet towards higher binding energies by 0.25 eV, the spin-orbit splitting did not change, which agrees with the literature data [19]. Moreover, an additional peak appears at energy of 135 eV, corresponding to the oxide form of phosphorus, presumably P_2O_5 . Also, islands with an altitude of about 5 nm and a width of 50 nm (Fig. 4b) were found in the AFM image of the surface of single crystals held in the air for several days. The islands, according to the published data [20], represent oxidized sections of the phosphorus surface.

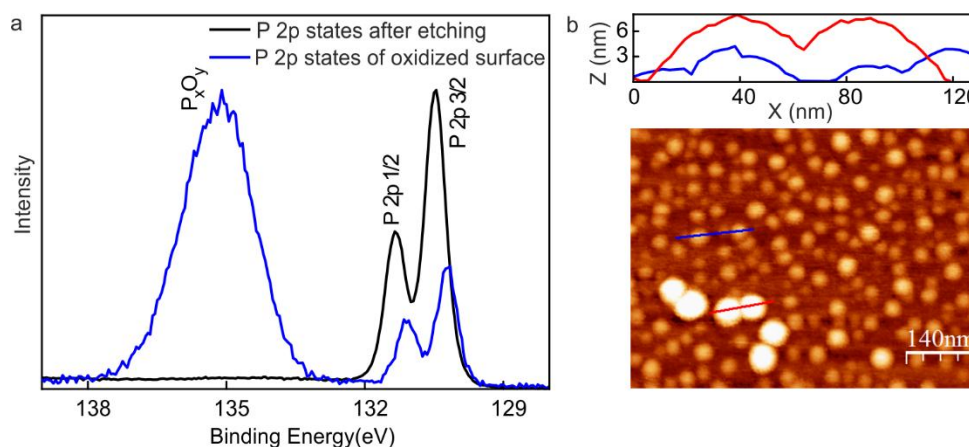


Fig. 6: a) Spectrum of the P2p states after etching and after exposure of the crystal under atmospheric conditions for 100 days, b) AFM image of the oxidized bP surface (inset: profiles along the lines).

Using the XPS method, the electronic structure of the valence band was studied. Figure 5b shows the spectra of the valence band for a pure and oxidized surface of single crystals of black phosphorus. In the spectrum of the pure surface of the P crystal, features are present at binding energies of 2.8, 5, 6.5, 11, and 14 eV. It can be seen that in the spectrum of a sample exposed under atmospheric conditions, peaks with binding energies of 2.8, 5, and 6.5 eV corresponding to black phosphorus are suppressed, and features in the range from 5 to 12 eV appear related to the oxidized form of phosphorus with a larger band gap.

To compare the experimental data, theoretical calculation of the density of states (DOS) by the density functional method was carried out (the lower curve in Fig. 5b). According to the calculations, the main contribution to the DOS in the range from 8 to 16 eV is made by 3s states, and that in the range from 1 to 8 eV is made by the 3p-state of phosphorus. It should be noted that qualitatively calculated spectra of the DOS are in a good agreement with the experiment.

For transport measurements, larger single crystals obtained by the gas transport reaction method were used, and on their basis three samples were prepared. Samples 1 and 2 were a black phosphorus single crystal on a sapphire substrate with “pressure” contacts (Fig. 7a). Sample 3 was a black phosphorus single crystal on a silicon substrate with deposited tungsten contacts (Fig. 7b). The contacts were applied by the method of a focused ion beam on Dual Beam VERSA 3D.

The measurements of the electrical resistance of samples 1 and 2 were performed using direct current by a four-contact method, the electrical conductivity and magnetoresistance of sample 3 were measured with alternating current.

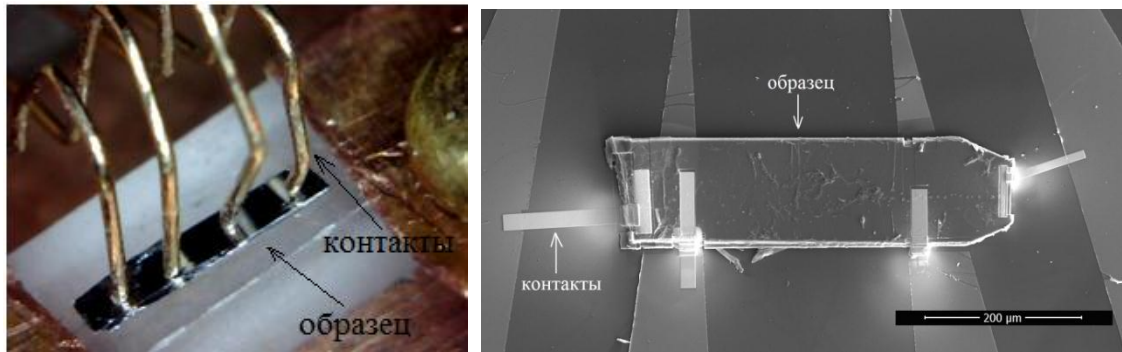


Fig. 7: "Spring" contacts (a) and contacts applied using FIB (b).

The direction of current in the samples coincided with the Y direction during the experiment. Fig. 9a shows a temperature dependence of the resistance of the synthesized single crystals.

The temperature interval below 300 K corresponds to the region of impurity conduction, and the resistance of the samples with an increasing temperature increases exponentially. The activation energy of the impurities, calculated from the temperature dependence of the resistance, was 10, 16 and 7 meV for samples 1, 2 and 3, respectively, which agrees with the literature data [8]. Fig. 8b demonstrates a temperature dependence of the electrical conductivity of sample 3 from 1.5 to 10 K. The measurements of the electrical conductivity versus temperature for samples 1 and 2 were performed up to 4.2 K, the data on these samples for temperatures below 20 K are given in the inset to the figure.

It can be seen that the temperature dependence of the electrical conductivity of sample 3 is linear in the logarithmic scale, which is characteristic of the regime of weak localization in the two-dimensional case. The results obtained are in agreement with the literature data published previously where two-dimensional contribution to the conductivity is observed in the weak localization regime [21].

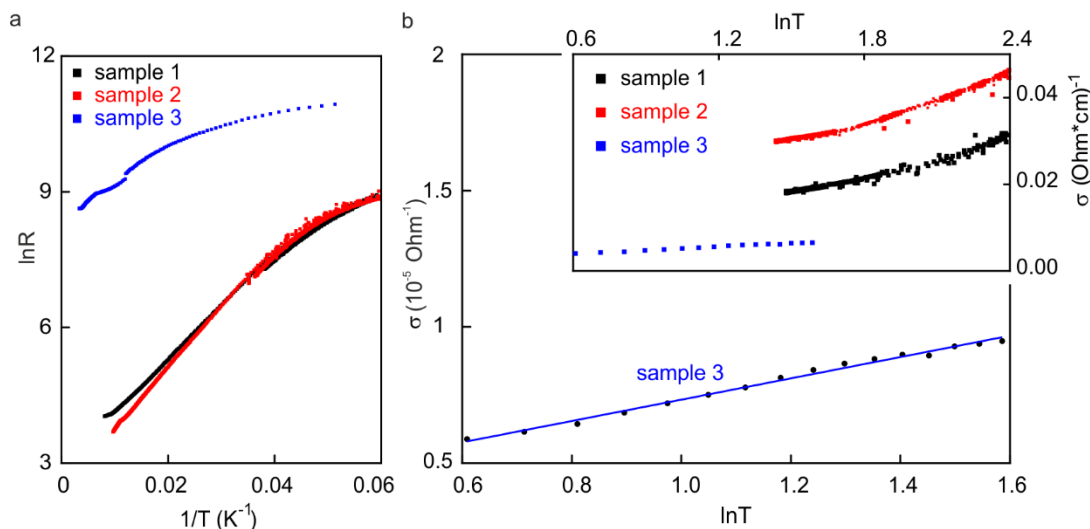


Fig.8: Temperature dependences of the resistance of the samples.

As is known, weak localization is detected by its destruction in a magnetic field due to a gradual decrease in the interference correction to the resistivity. Fig. 9 shows measurements of the magnetoresistance at $T=0.5$ K in a magnetic field up to 8T. The direction of current coincided with the Y direction, the magnetic field was applied perpendicular

to the planes of the layers along Z. It can be seen that in negative fields negative magnetoresistance is observed. When the magnetic field is turned on, the drop in resistance of sample 3 continues to the value of the magnetic field of 0.95T, after which, apparently, a complete destruction of weak localization occurs, and resistance increases.

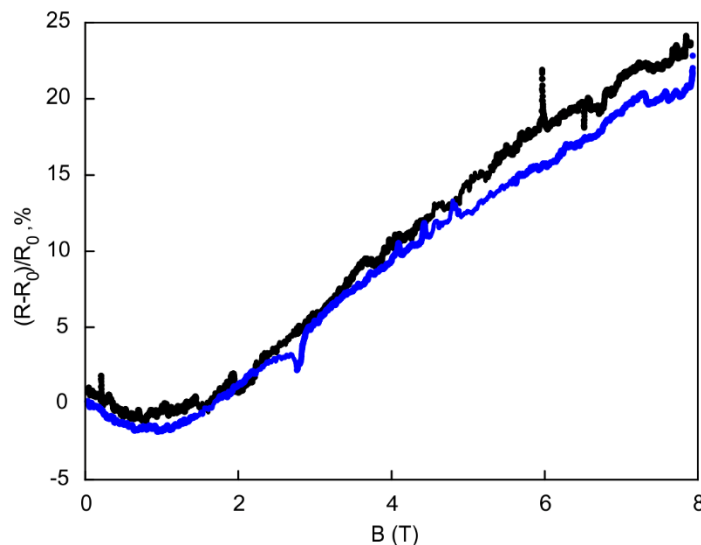


Fig. 9: Dependence of the resistance of sample 3 on the applied magnetic field (black curve ~ as the magnetic field increases, blue ~ when decreasing).

The mean free path calculated from the value of the magnetic field completely destroying the weak localization was about 26 nm. The maximum of the negative magnetoresistance was 1.8% at a field of 0.95T. At 8 Tesla, the magnetoresistance was 23%, the classical quadratic dependence on the magnitude of the magnetic resistance was not observed.

3. CONCLUSION

The conditions for synthesis of black phosphorus crystals have been optimized, single crystals have been obtained by high-pressure and gas-transport reaction methods. The electronic structure of the obtained crystals has been studied by the XPS method; the experimental data are in a good agreement with the theoretical results obtained by the DFT. The oxidized portions detected by ACM indicate oxidation of the black phosphorus surface when exposed to the air. The atomic resolution of the surface of a single crystal has been obtained by the STM method, and the estimate of the band gap (0.3-0.35 eV) for black phosphorus has been made from the tunnel spectra.

From the linear nature of the dependence of the electrical conductivity on the temperature in a logarithmic scale below 10K and the presence of negative magnetoresistance at 0.5K in magnetic fields from 0 to 0.95T it is assumed that a weak localization effect is observed in the two-dimensional case under these conditions.

Acknowledgments

The authors thank V.M. Chernyak, S.V.Chekamazov, A.S. Ksenz and R.N. Mozhchil for technical support of the experiments. The authors acknowledge support of the Research Facility Center at ISSP RAS. Funding of the State task of the Institute of Solid State Physics of the Russian Academy of Sciences is gratefully acknowledged.

REFERENCES

1. Liu, H., Neal, A. T., Zhu, Z., Luo, Z., Xu X., Tománek, D., Ye P.D., *ACS Nano*, **8**, 4033 (2014). doi: 10.1021/nn501226z.
2. Jingsi Qiao, Xianghua Kong, Zhi-Xin Hu, Feng Yang & Wei Ji, *Nature communications*, **5**, 4475 (2014).
3. Li L., Yu Y., Ye G. J., Ge Q., Ou X., Wu H. & Zhang Y. *Nature nanotechnology*, **9**, 372 (2014).
4. Yau S. L., Moffat T. P., Bard A. J., Zhang Z., & Lerner M. M., *Chemical physics letters*, **198**, 383 (1992).
5. Keyes R. W.. *Physical Review*, **92**, 580 (1953).
6. Warschauer D., *Journal of Applied Physics*, **34**, 1853 (1963).
7. Akahama Y., Endo S. & Narita S. I., *Journal of the Physical Society of Japan*, **52**, 2148 (1983).
8. Baba M., Nakamura Y., Takeda Y., Shibata K., Morita A., Koike Y., & Fukase T., *Journal of Physics: Condensed Matter*, **4**, 1535 (1992).
9. Takao Y., Asahina H., & Morita A., *Journal of the Physical Society of Japan*, **50**, 3362 (1981).
10. Goodman N. B., Ley L., & Bullett D. W., *Physical Review B*, **27**, 7440 (1983).
11. Cai Y., Zhang G., & Zhang Y. W., *Scientific reports*, **4**, 6677 (2014).
12. Liang L., Wang J., Lin W., Sumpter B. G., Meunier V., & Pan M., *Nanoletters*, **14**, 6400 (2014).
13. Bridgman P. W., *Journal of the American chemical society*, **36**, 1344 (1914).
14. Krebs H., Weitz H., & Worms K. H., *Zeitschrift für anorganische und allgemeine Chemie*, **280**, 119 (1955).
15. Brown A., & Rundqvist S., *Acta Crystallographica*, **19**, 684 (1965).
16. Lange S., Schmidt P., & Nilges T., *Inorganic Chemistry*, **46**, 4028 (2007).
17. Nilges T., Kersting M., & Pfeifer T., *Journal of Solid State Chemistry*, **181**, 1707 (2008).
18. Köpf M., Eckstein N., Pfister D., et al, *Journal of Crystal Growth*, **405**, 6 (2014).
19. Edmonds M. T., Tadich A., Carvalho et al, *ACS applied materials & interfaces*, **7**, 14557 (2015).
20. Kang J., Wood J. D., Wells S. A., Lee J. H., Liu X., Chen K. S., & Hersam M. C., *ACS nano*, **9**, 3596 (2015).
21. Baba M., Izumida F., Takeda Y., Shibata K., Morita A., Koike Y., & Fukase T., *Journal of the Physical Society of Japan*, **60**, 3777 (1991).